Conference on Modelling Fluid Flow (CMFF'25)
The 19th International Conference on Fluid Flow Technologies
Budapest, Hungary, August 26 - August 29, 2025

MOBILE SEPARATION OF COMPLEX OIL-WATER MIXTURES WITH AN ADAPTED PITOT PUMP

Jessica DAFIS[1], Xuemei ZHANG[2], Katharina ZÄHRINGER[3]

[1]Corresponding Author. Laboratory of Fluid Dynamics and Technical Flows, Otto von Guericke University Magdeburg, Universitätsplatz 2 39106 Magdeburg, Germany. Tel.: +49 391 67-52539. E-mail: jessica.dafis@ovgu.de
[2] State Key Laboratory of Multiphase Flow in Power Engineering, Xi'an Jiaotong University, Xi'an, China.
[3] Laboratory of Fluid Dynamics and Technical Flows, Otto von Guericke University Magdeburg, Germany. E-mail: zaehringer@ovgu.de

ABSTRACT

Oil-water (o/w) mixtures are found in numerous applications, mainly for processes, chemical and environmental engineering. Whenever oil-containing phases are utilized, the wastewater is often contaminated with oil, and these emulsions can cause significant environmental problems even at low concentrations e.g., polluting water bodies and damaging aquatic ecosystems.

The use of water treatment systems (e.g., the PTJ separating pump described below) is therefore essential in order to reliably remove the oil from the wastewater. In order to improve oil-water separation systems in a reliable manner, concentration measurements must also be accurate. The current study investigates the improvement of accuracy and reliability of o/w concentration measurements. A fluorescence-based imaging method has been developed to quantify the o/w concentration, especially in the relevant, low concentration ranges (5 mg/l to 200 mg/l). This method uses the fluorescent dye *Nile red (CAS-Number: 7385-67-3)*, acquires high-resolution images and analyses the droplet size and fluorescence intensity.

Using these concentration measurements, an existing laboratory test rig is improved in terms of pressure increase, and the control unit is miniaturized in order to convert the lab system into a mobile unit that can be used on-site in case of disasters.

NOMENCLATURE

Latin letters

FS	[-]	flow-split
g	[m s^{-2}]	gravitational acceleration
H_{HPO}	[m]	pressure head
$\dot{m}$	[kg s^{-1}]	mass flow rate
p	[Pa]	static pressure
n	[rpm]	rotational speed
m	[-]	Gradient
k	[-]	Intersection
T	[°C]	Temperature

Greek letters

α	[-]	oil concentration
ρ	[kg m^{-3}]	mixture density

Abbreviations

CF	Coriolis mass flowmeter
HPO	High-Pressure Outlet
LPO	Low-Pressure Outlet
o/w	oil-water
ppm	parts per million (=mg/l)
rpm	revolutions per minute
PTJ	Pitot-Tube Jet (pump)
RoI	Region of Interest

1. ENVIRONMENTAL CHALLENGES OF OIL SPILLS

Water pollution, especially caused by oil spills, remains a significant challenge for society. Given the increasing shortage of drinking water and the rising frequency of environmental disasters, finding effective clean-up solutions is more important than ever [1].

Although the *Deepwater Horizon* spill in 2010, which released 800 million litres of crude oil into the Gulf of Mexico, is the most well-known case, there are numerous other examples of oil pollution in daily life [2,3]. Industrial processes, shipping, and the uncontrolled discharge of bilge oil at ports or through accidents at sea significantly contribute to oil pollution [4]. However, this issue is not limited to oceans — inland waters such as lakes, rivers, and even groundwater can also be polluted. Heavy rain events like floods and high tides destroy houses, vehicles, and machinery containing oils, fuels, and other pollutants, thus threatening groundwater through contamination [4,5].

Standard oil spill control methods, such as barrier systems, chemical dispersants, and

(controlled) burning, often have limited effectiveness and can even worsen environmental damage [6]. Therefore, innovative approaches are urgently needed to quickly and effectively separate oil from contaminated water, enabling the rapid return of cleaned water to water bodies [7].

2. THE LABORATORY PITOT-TUBE JET PUMP FOR OIL-WATER SEPARATION

To deal with environmental problems and remove oil spills quickly and cost-effectively on site the *Chair of Fluid Mechanics and Technical Flows* has developed a mechanical separation method based on a rotating pump system. The modified Pitot-Tube Jet (PTJ) pump is an innovative solution for oil-water separation while simultaneously transporting the two separated phases [8–11]. With the PTJ pump it is possible to achieve significant success in the separation of oil-contaminated water. Laboratory analyses demonstrated a water purity below 2 to 5 ppm, which is a sufficient level to allow the purified water to be discharged directly into the environment.

The name of the Pitot pump comes from Henri Pitot. The Pitot tube extends in radial direction from the rotation axis almost up to the inner wall of the rotor. At this point, the liquid reaches its highest velocity and enters the Pitot tube. As a standard pump system, the Pitot tube has one inlet and one outlet. To adapt the system for separating oil-water mixtures, the Pitot tube was modified to involve one inlet for the oil-water mixture, and two outlets for the separately discharged liquids.

Figure 1 shows the modified Pitot tube inside the small-scale laboratory centrifuge. In first experiments, the system operates without blades and functions purely as a centrifuge. In this setup, the pressure increase results only from rotation and from the pressure build-up inside the Pitot tube, working as a diffusor. Within the Pitot tube, the high kinetic energy of the accelerated fluid is converted into usable pressure energy. In this way, the Pitot tube functions similarly to a volute casing in a classical centrifugal pump.

The incoming o/w mixture is separated in the rotor by centrifugal forces. The heavier phase (water) is pushed towards the outer rotor walls, while the lighter phase (oil) collects in the core, close to the axis of rotation. As a result, the water exits through the head of the Pitot tube, where it experiences a pressure increase before being expelled through the High-Pressure Outlet (HPO), while the oil exits through the second, central outlet, the Low-Pressure Outlet (LPO).

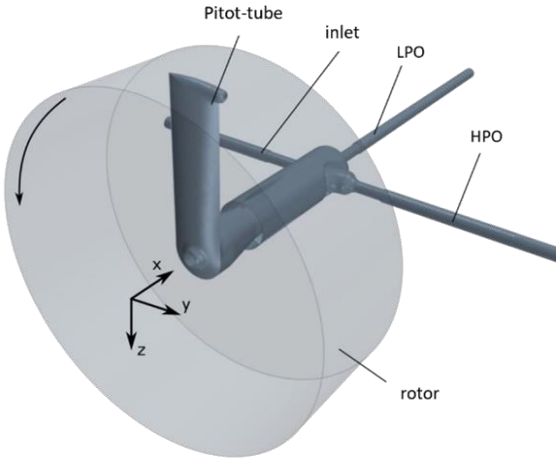

Figure 1: Schematic image of the modified Pitot tube in the lab-scale PTJ.

While combining pumping and separation, the PTJ pump achieves efficient oil-water purification at high flow rates, making it suitable for wastewater treatment in natural environments.

3. EVALUATION OF O/W CONCENTRATION AND PRESSURE

To investigate and optimize the PTJ pump, a laboratory-scale experimental setup was developed and constructed. Connected pipelines and valves ensure that the incoming liquids can be tested under various inflow conditions. The system allows the analysis of different oils and contaminants. For standard tests, sunflower oil is used first for safety reasons. In advanced tests, mineral or synthetic oils and fuels can also be examined. A selection of the tested substances is listed in Table 1. Water is always present as a component, while the oil phases vary.

Table 1: Densities of different fluids tested in the laboratory test rig [12–15]

	Density at ~ 20°C [kg·m^{-3}]
Water	998
Sunflower Oil	918 – 923
Olive Oil	910
Rapeseed Oil	907
Engine Oil	855 – 907
Gasoline	720 – 767
Diesel fuel	802 – 886
Heating Oil	815

Due to differences in density, the separation process varies depending on the type of oil. Mineral and synthetic oils have a greater density difference from water, making them easier to separate. In contrast, vegetable oils such as sunflower oil have a much smaller density difference, which makes their separation more difficult from a physical perspective. While sunflower oil is preferred to limit safety concerns and facilitate handling, it presents a

more challenging separation scenario compared to mineral oils.

Using the schematic experimental setup shown in Figure 2, the key parameters – o/w concentration at the HPO (α_{HPO}) and pressure buildup (H_{HPO}) - can be analysed and evaluated. This allows the identification of relevant parameter ranges and the optimization of the system in order to improve performance.

The *mass flow* ($\dot{m}$), *density* (ρ), and *temperature* (T) are measured during the tests using Coriolis flow meters (CF). The operating principle is based on the controlled generation of Coriolis forces, which occur when translational and rotational movements are superimposed in a system. For pressure measurements, *Cerabar T PMP131* pressure sensors from *Endress & Hauser* are used. The process pressure influences the metal membrane of the sensor. The signal is transmitted to the resistance bridge through a filling liquid. The pressure is determined based on the pressure change, which is proportional to the bridge output voltage. The configuration of the measuring devices is shown in the schematic test setup.

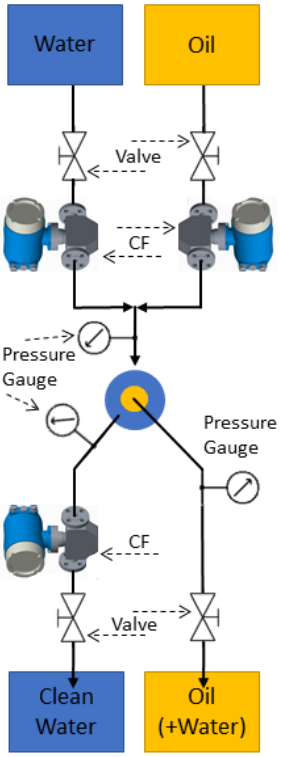

Figure 2: Experimental test setup of the PTJ pump on pilot scale.

The oil concentrations at the HPO and LPO are calculated using the corresponding densities. The correlation can be derived from equations (1a) and (1b). An oil concentration of 0.1 means that oil constitutes 10% of the mass of the mixture.

$$\alpha_{\mathrm{HPO}} = \frac{\rho_{\mathrm{HPO}} - \rho_{\mathrm{Water}}}{\rho_{\mathrm{Oil}} - \rho_{\mathrm{Water}}} \qquad (1a)$$

$$\alpha_{\mathrm{LPO}} = \frac{\rho_{\mathrm{LPO}} - \rho_{\mathrm{Water}}}{\rho_{\mathrm{Oil}} - \rho_{\mathrm{Water}}} \qquad (1b)$$

The measured pressure is converted into the pressure head using equation (2). This represents the height that the pump may have to overcome in order to pump the separated mixture at the accident site if there are barriers to deal with.

$$H_{\mathrm{HPO}} = \frac{\Delta p}{\rho_{\mathrm{HDA}} g} \qquad (2)$$

4. EXPERIMENTAL OPERATION

In previous tests, the operating parameters were adjusted to define the optimum separation ranges. However, due to measurement inaccuracies in the Coriolis flow meters, these parameter limits need further refinement to ensure consistent and optimal separation performance across the full operating range.

The operating parameters include the rotational speed, the mass flow rate at the inlet, the oil concentration at the inlet and the flow split. These parameters define a specific operating point, and variations in these parameters have a direct effect on the two main objectives. Depending on the geometric configuration, the effect of each parameter on these targets varies, resulting in shifts of the operating limits of the system.

In the first tests, a rotor without blades was used, operating as a pure centrifuge, as seen in Figure 3a. Later on, the rotor was modified with a blade geometry that only rotates in the water phase (Figure 3b). This modification was intended to increase the pressure within the system and at the same time prevent the formation of emulsions inside the rotor, which would otherwise affect an efficient separation.

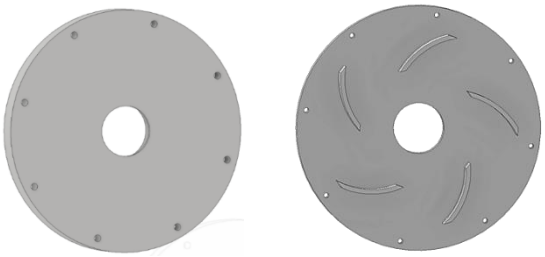

Figure 3: (a) Front of the rotor without blade geometry and (b) with adapted blades that only rotate in the water phase (close to periphery).

A comparison of the pressure increase as a function of the speed shows that a plate with blades generates a higher pressure build-up than the pure centrifuge configuration. As can be seen in Figure 4, the pressure head increases with rotational speed for both geometries. In the configuration with blades, however, the oil concentration, given in the respective boxes in the curves, also increases, which corresponds to a decrease in separation efficiency.

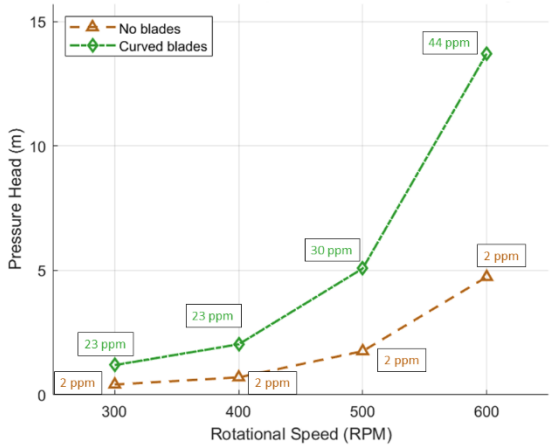

Figure 4: Pressure build-up as a function of rotational speed without blades (orange) and with adapted blades (green). The final oil concentration for each case is given in the respective boxes.

As a result, the parameter limits must be redefined and tightened. Another possibility is that the geometric configuration needs to be further optimized. As the oil concentrations in this system are so low that they cannot be accurately measured by the Coriolis flow meters, samples of the purified water were taken directly from the system and sent to the laboratory for analysis using the TOC (Total Organic Carbon) method.

Although this method is very accurate, it is also very time-consuming. Only a limited number of samples can be analysed, which makes it difficult to vary the parameters and leads to a slow and costly optimization process.

Since the mass balance method is no longer suitable for accurately determining the operating limits and optimizing the system due to the very low permissible oil concentrations in the treated water, a faster and more precise method must be developed to support system optimization.

5. MEASURING THE OIL-WATER CONCENTRATION USING A FLUORESCENT DYE

A better approach for reliably measuring oil concentrations in the range of 5 to 500 ppm has thus been developed. The measurement principle relies on fluorescence imaging of the dyed emulsion.

A requirement for this method is the ability to detect fluorescence signals from the mixture. Aromatic molecules show fluorescent properties. Each substance has a characteristic range of wavelengths at which absorption and fluorescence emission occur.

The oils listed in Table 2 have different fluorescence properties. While vegetable oils generally require excitation in the UV range, mineral oils show an emission peak with excitation in the wavelength range of around 420-490 nm. The sunflower oil used as a standard in the experiments has very weak fluorescence signals. Therefore, the sunflower oil is inoculated with a selective fluorescent dye tracer - *Nile red* (*CAS No. 7385-67-3)* - at a concentration of 1 mg/l in the oil. This tracer is insoluble in water and serves as an effective marker for the oil droplets. The typical absorption and fluorescence spectra of Nile red are shown in Figure 5.

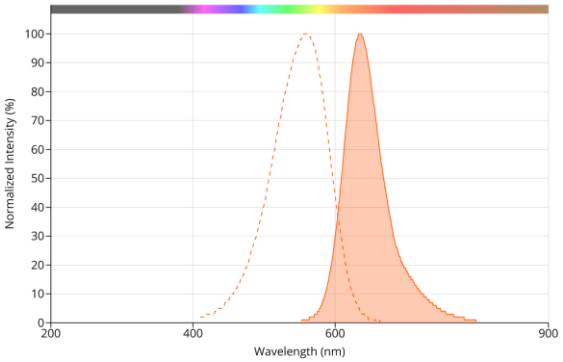

Figure 5: Absorption and fluorescence spectra of Nile red [16]

To simplify further processing, a stock solution of oil and the fluorescent dye Nile red was prepared. For 1 litre of sunflower oil, a mass of 1 mg Nile red was used. The dye, initially in powder form, was thoroughly mixed with the oil until fully dissolved. To ensure a consistent signal, the oil-dye mixture was filtered before being mixed with water to remove any residual solids.

Both, the pure sunflower oil and the oil solution with added *Nile Red* were analysed using a *Horiba Duetta* spectrometer. A 3D fluorescence spectrum was generated, as shown in Figures 6 and 7. The signals from pure sunflower oil are very weak and may not be strong enough for a calibration curve to highlight differences between different concentrations. On the other hand, for the dyed sunflower oil, excitation at a wavelength of 535 nm shows an emission peak at 570 nm.

To set up the experimental system, the excitation wavelength was selected based on the fluorescence spectra, with a green LED chosen as the excitation source. The LED used is a multicolor LED that can emit green, blue, or red light depending on the voltage applied. The blue LED is particularly suitable for further experiments with mineral oils, as these oils do not require the addition of a fluorescent dye. Non-toxic olive oil can also be excited in the red wavelength range and, therefore, can be used for further investigations.

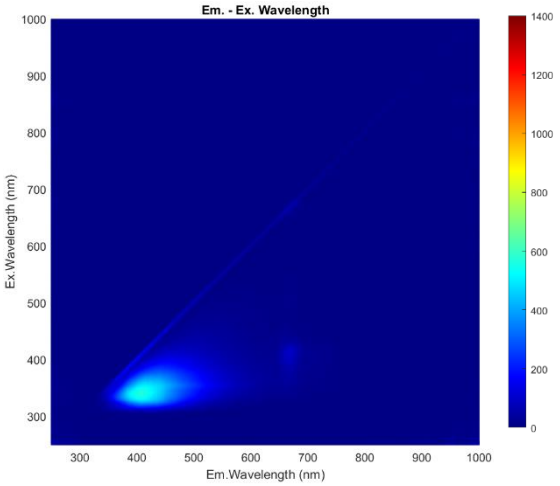

Figure 6: Excitation and emission wavelengths of pure sunflower oil, showing the fluorescence signal.

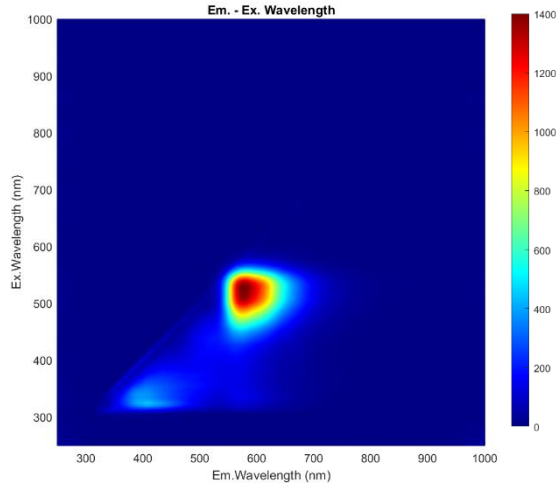

Figure 7: Excitation and emission wavelengths of sunflower oil seeded with 1 mg/l Nile red, showing the fluorescence signal.

6. EXPERIMENTAL SETUP FOR FLUORESCENCE MEASUREMENTS

The fluorescence-based methodology for oil-water (o/w) measurements relies on the presence of a stable and reproducible emulsion.

Generating a stable oil-water mixture without emulsifiers requires high-energy mixing to create fine, dispersed oil droplets. A stable emulsion is essential because fluorescence imaging depends on homogeneously distributed oil droplets for reliable quantification. In this study, a *Polytron PT3100* homogenizer was used, capable of handling up to 2 liters of total volume at a maximum rotational speed of 12,000 rpm. However, even at this speed, the emulsion remained stable for only about three minutes, requiring rapid measurements before phase separation begins. The preparation process was standardized for all experiments.

A volume of 200 ml of deionized water was mixed with a controlled amount of dyed sunflower oil to obtain the desired o/w concentration. The mixtures were dispersed at a rotational speed of 12,000 rpm for 120 seconds.

After the emulsification process, the samples were transferred into disposable cuvettes. These samples were positioned in front of a CMOS camera (*FLIR Blackfly S*, 5 MP), equipped with a *Nikon F60* objective lens (f-number: 2.8, scale factor: 59.7 pixels/mm). All measurements were performed with a constant exposure time of 5000 µs.

For fluorescence excitation, two LEDs (emission peak: 535 nm) were positioned on either side of the cuvette. This setup ensured intense and continuous illumination, crucial for uniform fluorescence excitation. Additionally, black shielding was used to minimize the entry of ambient light, as shown in Figure 8. The images were saved and later used for image processing.

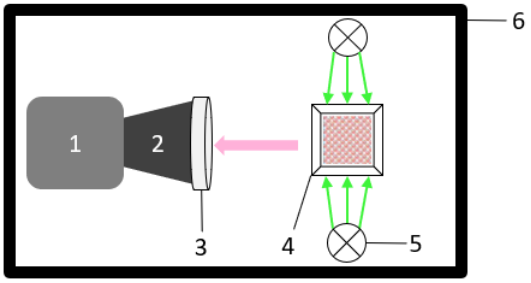

Figure 8: Schematic setup of the fluorescence imaging methodology for o/w concentration measurements [17]

Table 2: Components of experimental setup

1	CMOS camera (Mono, 5MP, 16 bit)
2	Objective lens
3	High-pass filter
4	Cuvette (Oil in water emulsion with Nile red)
5	LED illumination
6	Housing to avoid disturbing light

For image processing, a simple image-analysis algorithm was coded using *Matlab (Version R2019, The MathWorks Inc.)*. The image processing sequence begins by reading the raw images, which are captured as grayscale images (Figure 9).

The grayscale intensity is directly proportional to the fluorescence signal produced by the sample illuminated in the cuvette. Subsequently, a Region of Interest (RoI) is automatically set. This step is necessary to avoid regions with strong optical distortion near the edges of the cuvettes.

Figure 9: Image of the cuvette taken with the *FLIR* camera. RoI marked with a red rectangle.

Since all cuvettes were placed in exactly the same position, the RoI always corresponds to identical pixel regions within the image: 400 pixels in the x-direction (horizontal) and 500 pixels in the y-direction (vertical), resulting in a total of 200,000 pixels. Grayscale intensities (average pixel intensity) and distribution (standard deviation of pixel intensity) were evaluated for this area.

Finally, the resulting intensity value is correlated with the known o/w concentration.

7. RESULTS

A concentration-dependent calibration curve was created based on the measurement setup described in Section 6. Figure 10 shows the correlation between the o/w concentration and the mean fluorescence intensity of the samples.

It can be observed that each oil concentration corresponds to a specific fluorescence intensity value. This relationship allows for the determination of the oil content in the water based on the measured fluorescence intensity, provided that the dye concentration is known (here: 1 mg/l *Nile red* in oil).

This linear correlation enables the fitting of a regression curve through the measured data points and facilitates the quantitative determination of the oil concentration in the water based on the fluorescence intensity. The following equation can be derived from this linear relationship:

$$y = m \cdot x + k \qquad (3)$$

Where y is the fluorescence intensity and x is the oil-water concentration. *Matlab* is used to determine the gradient m and the intersection k on the y-axis. The values obtained for the regression line are:

- Intersection (k) = 403.56
- Gradient (m) = 24.81

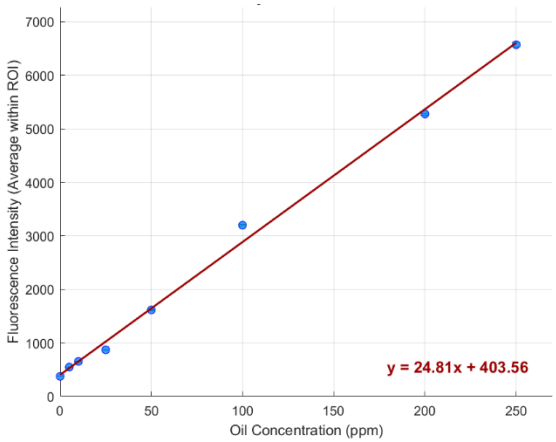

Figure 10: Fluorescence intensity as function of o/w concentration.

This results in the following equation:

$$I = 24.81 \cdot c_{o/w}\,[\text{ppm}] + 403.56 \qquad (4)$$

This equation can be converted to solve c and calculate the oil concentration in the water based on the measured fluorescence intensity. Provided that the dye concentration of 1 mg/l *Nile Red* is known.

$$c_{o/w}[\text{ppm}] = \frac{I - 403.56}{24.81} \qquad (5)$$

8. EXTENSION OF FLUORESCENCE IMAGING WITH MICROSCOPIC ANALYSIS

While a correlation between fluorescence intensity and oil concentration has already been demonstrated, the next step is to investigate the behaviour of the oil droplets in the emulsion as the o/w concentration increases. For this purpose, a second *FLIR* camera was used, and *the Questar QM-1 Long Distance Microscope* (7) was integrated into the experimental setup to investigate the microscopic properties of the emulsion. The extended experimental setup is shown in Figure 11. All other test parameters remained constant.

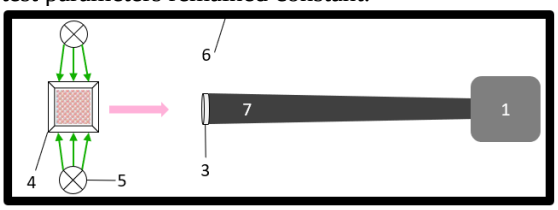

Figure 11: Schematic setup of the fluorescence imaging methodology with microscope analysis

With the long-range microscope, the oil droplets become visible through the fluorescent dye and enable a detailed examination. While the average fluorescence intensity can still be evaluated, the main focus is now on the formation of the droplets and their number as a function of the oil concentration. A

microscope image of the droplets can be seen in Figure 12.

Matlab is used to analyse the number of droplets. A contrast threshold is defined in the script in order to consider only the droplets within a certain focus plane.

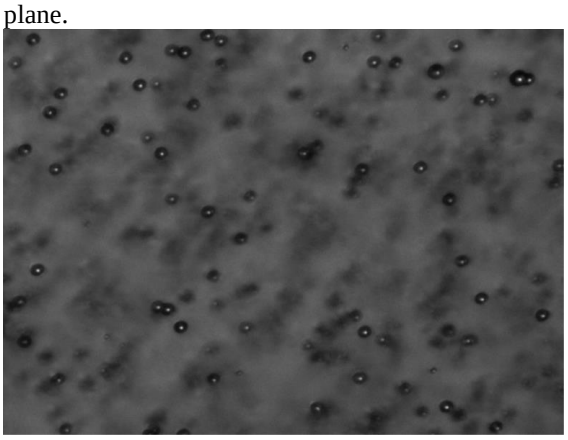

Figure 12: Droplet distribution for 50 ppm o/w

The series of experiments described above was repeated. This time, however, fluorescnence images and microscopic images were taken simultaneously. The analysis of the number of droplets as a function of the oil concentration in water is shown in Figure 13.

While the fluorescence image analysis showed a linear correlation between oil concentration and fluorescence intensity, a correlation between droplet number and oil concentration can also be observed in the microscopic images. However, no linear correlation can yet be derived from the microscopic data. These results clearly show the potential of microscopic studies, but further optimization of both image quality and analysis script are required to accurately count and analyze the droplets. Such improvements could lead to a better understanding of the relationship between oil concentration and droplet behavior.

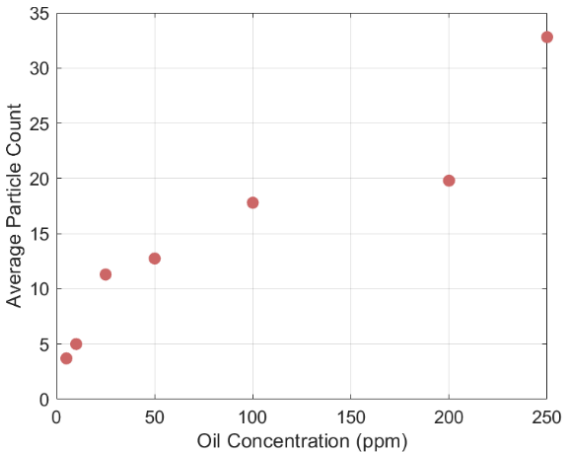

Figure 13: Dependence of the number of particles on the oil concentration.

8. CONCLUSIONS & FUTURE APPLICATIONS

The separation of oil-water mixtures is still a major challenge, especially in environmental protection and industrial applications. The modified PTJ pump presented in this study offers a promising solution by combining centrifugal forces with a pumping mechanism to improve the efficiency of oil-water separation systems. Laboratory tests have shown that this system can achieve a water purity level below 5 ppm, which meets the requirements for the discharge of water in the environment.

One of the biggest challenges in optimizing the PTJ system is the accurate and rapid measurement of the oil-water concentration. While laboratory testing provides highly accurate results, it is time consuming and impractical for real-time testing under field operating conditions, especially given the variability of system parameters. While the in-line method (CF measurement/density mass balance) provides fast results, they lack the accuracy required for precise monitoring below 1000 ppm. Therefore, a fluorescence-based measurement technique using the dye Nile red was introduced in this study as a reliable and fast alternative.

This fluorescence measurement method offers a sample-based evaluation that provides rapid results (a few minutes from sampling to oil concentration determination). A calibration curve for oil concentrations from 5 ppm to 500 ppm has been developed. Good correlations between droplet size and oil concentration have also been demonstrated. Nevertheless, there are still challenges and a need to optimize the microscopic analysis in order to increase accuracy, especially in the lower concentration ranges.

Both methods need also to be further developed to obtain an in-line approach in the future, providing hopefully real-time response times.

According to the results of the present study, it is possible to arrange all components of the set-up in such a way that in-line measurements are possible. However, the calibration function shown in Figure 10 is only valid if all optical and system parameters are kept unchanged. This means that the camera and illumination settings as well as the distances between the individual components in the in-line setup must be identical to the offline setup. In addition, all the oil in the reservoir of the pilot plant must be inoculated at the same *Nile red* concentration (1 mg/l) as before.

In addition, the image processing algorithm, which currently runs in a sequential mode as post-processing after image acquisition, needs to be modified to enable simultaneous image acquisition and processing as a real-time process. This will ultimately enable the development and implementation of a feedback control for the PTJ pump. Such a control is necessary in order to react to

transient process conditions resulting from a fluctuating oil concentration at the inlet, for example.

ACKNOWLEDGEMENT

This project is funded by the (DBU) under the grant number 38123/01 – 23.

We would also like to thank the UFZ Leipzig, in particular Jonas Köhne, for his active support with the sample analyses.

REFERENCES

[1] Sousa, A. M., Pereira, M. J., & Matos, H. A. (2022). *Oil-in-water and water-in-oil emulsions formation and demulsification*. Journal of Petroleum Science and Engineering, **210**, 110041.

[2] Hu, C., Herz, C., & Hartman, R. L. (2013). *Microfluidic dispersion of mineral oil-seawater multiphase flows in the presence of dialkyl sulfonates, polysorbates, and glycols*. Green Processing and Synthesis, **2**(6), 611–623.

[3] Overton, E. B., Adhikari, P. L., Radović, J. R., & Passow, U. (2022). *Fates of petroleum during the Deepwater Horizon oil spill: A chemistry perspective*. Frontiers in Marine Science, **9**.

[4] Singh, B. J., Chakraborty, A., & Sehgal, R. (2023). *A systematic review of industrial wastewater management: Evaluating challenges and enablers*. Journal of Environmental Management, **348**, 119230.

[5] Al-Majed, A. A., Adebayo, A. R., & Hossain, M. E. (2012). A sustainable approach to controlling oil spills. Journal of Environmental Management, **113**, 213–227.

[6] Peterson, C. H., Rice, S. D., Short, J. W., Esler, D., Bodkin, J. L., Ballachey, B. E., & Irons, D. B. (2003). Long-term ecosystem response to the Exxon Valdez oil spill. Science, **302**(5653), 2082–2086.

[7] Kwon, G., Kota, A. K., Li, Y., Sohani, A., Mabry, J. M., & Tuteja, A. (2012). On-demand separation of oil-water mixtures. Advanced Materials, **24**(27), 3666–3671.

[8] Meyer, J. (2019). *Optimierung einer Pitot-Pumpe und deren Adaption zur Öl-Wasser-Trennung* (Ph.D. thesis). University of Magdeburg.

[9] Meyer, J., & Thévenin, D. (2016). *Proceedings of the 9th International Conference on Multiphase Flow*, Firenze, Italy.

[10] Meyer, J., Daróczy, L., & Thévenin, D. (2017). *Shape optimization of the pick-up tube in a Pitot-tube jet pump*. Journal of Fluids Engineering, **139**, 021103/1–11.

[11] von Deylen, J., Köpplin, J., & Thévenin, D. (2022). *Development and validation of a design tool for an improved Pitot-tube jet-pump allowing continuous fluid-fluid separation*. Journal of Fluids Engineering, **144**(7), 071401/1–11.

[12 NIST Standard Reference Database 69. (2008). *Thermophysical properties of fluid systems: Isobaric properties for water*.

[13] Federation of German Heating Industry (BDH). (2021). *Fuel heating oil EL: Information sheet No. 50*. https://www.bdh-industrie.de/downloads#technische-infoblaetter

[14] Park, S. H., Youn, I. M., Lim, Y., & Lee, C. S. (2013). *Influence of the mixture of gasoline and diesel fuels on droplet atomization, combustion, and exhaust emission characteristics in a compression ignition engine*. Fuel Processing Technology, **106**, 392–401.

[15] Ichu, C. B., & N., H. (2019). *Comparative study of the physicochemical characterization and quality of edible vegetable oils*. International Journal of Research in Information Science and Application Technology, **3**(2), 1–9.

[16] AAT Bioquest. (2025). *Spectrum [Nile red]*. Retrieved February 11, 2025, from https://www.aatbio.com/fluorescence-excitation-emission-spectrum-graph-viewer/nile_red

[17] Köpplin, J., Bednarz, L., Hagemeier, T., & Thévenin, D. (2021). *Fluorescence imaging methodology for oil-in-water concentration measurements*. Chemical Engineering & Technology, **44**(7), 1343–1349.